Estimation of Time-varying Frequency and its Rate of Change in Low-inertia Power Systems

Peng Li
School of Mechanical Eng. & Automation
Harbin Institute of Technology, Shenzhen
Shenzhen, China
lipeng2020@hit.edu.cn

Boli Chen
Dept. of Electronic & Electrical Eng.
Unniversity College London
London, United Kingdom
boli.chen@ucl.ac.uk

Zhongda Chu
Dept. of Electrical & Electronic Eng.
Imperial College London
London, United Kingdom
z.chu18@imperial.ac.uk

Aiguo Wu
School of Mechanical Eng. & Automation
Harbin Institute of Technology, Shenzhen
Shenzhen, China
agwu@hit.edu.cn

Fei Teng
Dept. of Electrical & Electronic Eng.
Imperial College London
London, United Kingdom
f.teng@imperial.ac.uk

Abstract—In this paper, a hierarchical estimation scheme is designed to track the frequency and its rate of change of non-stationary power signals. The frequency is retrieved by a kernel-based parameter estimator in the first step. Subsequently, the frequency estimates are injected into a kernel-based numerical differentiator to extract its changing rate. Thanks to the deployed Volterra integral operator and suitably designed kernel-functions, the proposed estimator can achieve very fast convergence speed without compromising the robustness against noise. Therefore, the real-time estimates are able to follow the time-varying frequency and its rate of change with satisfactory accuracy. The effectiveness and robustness of the proposed method are verified by numerical experiments considering typical practical scenarios under the disturbance of noise. The results of the proposed method are compared with a highly-concerned quadrature phase-locked-loop (QPLL) method.

Index Terms—component, formatting, style, styling, insert

I. INTRODUCTION

The frequency and its rate of change (RoCoF) are both significant criteria that characterize the qualitative behavior of power systems. Especially in recent years, new modes of RoCoF variation of the power network emerges with the development of new energy resources, such as wind and solar energy, bringing considerable challenges to grid stability maintenance. Therefore, fast and accurate estimation of frequency and RoCoF is urgently demanded. As such, effective frequency control and protection strategies, such as inertia emulation, can be applied promptly before potential malfunction have a chance to destabilize the power network.

Being a crucial estimation problem in both the engineering and scientific field, a large variety of frequency estimation algorithms have been proposed in the literature. Among them, the zero-crossing-based techniques (see [1]) are the most commonly used in the power system industry but they are vulnerable to disturbance and sudden frequency change. Alternatively, the discrete Fourier transform (DFT) is commonly concerned due to its simple structure and effectiveness while dealing with stationary signals. On the other hand, the adaptive-notch-filtering method (ANF) [2], [3] and frequency-adaptive Phase-Locked-Loop (PLL) [4], [5] still represent the most used approaches in power-electrical systems for their ease of implementation in digital signal processing platforms and its robustness to environmental and measurement noise.

Despite the rich literature on stationary frequency estimation, the persistent tracking of a time-varying frequency remains a challenging problem, which is the foundation for the detection of RoCoF, being also a crucial topic for modern power systems. In [6], the RoCoF is treated as a state variable of a dynamic system alongside with the frequency and both of the them are estimated in one step by a quadrature PLL (QPLL) resorting to several filtering techniques. More recently, in [7], it has been claimed that one-step methods tend to result in larger estimation error, in terms of Cramer Rao bounds, than estimating the frequency and RoCoF by separate steps. In this regard, an IDFT-based frequency estimator is proposed followed by a differentiator achieved by a Kalman filter. As discussed in [7], the trade-off between accuracy and latency of estimation is commonly seen, existing also in [6], [8]. Therefore, being a practically significant, fast, and accurate track of typical kinds of frequency and RoCoF variation is still an open problem that is worth exploring.

In the context of fast and accurate schemes, the finite-time estimation methods have drawn a wide range of concerns. In recent decades, multiple estimation methodologies have been proposed with the guarantee that the estimation error converges in finite time. Among them sliding mode methods [9], algebraic method (see [10], [11]), modulating function methods [12], kernel-based method [13] are the most renowned ones. Remarkably, all the above methods have found their applications in the frequency estimation of stationary signals. However, such methods are seldom explored for frequency-varying signals under the effect of noise.

In this paper, a two-step estimation scheme is designed to track both the frequency and RoCoF of a non-stationary signal. The estimator is based on the Volterra integral operator with specialized kernel functions, which have been proved to be an effective tool for fast and robust state and parameter estimation [14], [15]. Moreover, thanks to the exponential shape of the kernel function, it has been analyzed that the kernel-based estimators are capable of tracking time-varying frequency and RoCoF under certain practically reasonable assumptions.

Numerical validations are performed with comparisons to a well-known QPLL method in the presence of both simulated and experimental frequency variation modes to verify the effectiveness of the proposed scheme. The main contribution of the paper is twofold: 1) the development of the new and fast estimation scheme for tracking time-varying frequency and RoCoF, and 2) performance evaluation under practical operation conditions with comparisons to QPLL. It shows that the proposed algorithm can achieved negligible latency that appears in most of the existing methods.

This paper is organized as follows. Section II introduces frequency and RoCoF estimation problem in power systems. The proposed estimation scheme is described in Section III-A. Section IV presents numerical examples and comparisons, followed by the concluding remarks in Section V.

II. PROBLEM FORMULATION AND PRELIMINARIES

Consider a power signal

$$y(t) = A\sin(\omega(t)t + \phi_0), \tag{1}$$

where ϕ_0 is the initial phase angle, A is the amplitude of the signal, and $\omega(t)$ is the time-varying frequency. The RoCoF, denoted as $R_f(t)$, is defined by: $R_f(t) = \dot{f}(t) = \frac{\dot{\omega}(t)}{2\pi}$.

In practice, it is essential to capture abnormal RoCoF changes in order to deliver required control actions in case of safety hazards, such as frequency instable. Considering the unexpected RoCoF changes happen at $t = t_d \in \mathbb{R}_{\geq 0}$, the objective of this paper is to design a frequency and RoCoF estimator with fast response speed to the frequency and RoCoF changes, so that effective control or protection efforts, such as synthetic inertia, can be triggered and delivered to mitigate potential stability problem within a short time interval $t \in [t_d, t_0]$. Considering the short time interval and comparatively small value of $R_f(t)$, for a easier characterization, the variation of the angle is approximated to be linear in time increments, i.e. $\omega(t)t + \phi_0$. For further discussion, following assumptions are useful for the proposed estimation scheme.

Assumption 1 *Considering the practical circumstance of the power system, it is reasonable to assume the frequency (the angular velocity), the RoCoF and its rate of change remain bounded [7], such that there exists positive M_i ($i = 1, 2, 3$), such that*

$$\|f(t)\| \leq M_1, \quad \|R_f(t)\| \leq M_2, \quad \left\|\dot{R}_f(t)\right\| \leq M_3.$$

Assumption 2 *The value of the RoCoF is much smaller than the operational angular frequency, i.e. $\dot{\omega}(t) \ll \omega(t), \forall t \geq 0$, and the time required to accommodate unexpected RoCoF changes is small enough as compared to the value of the fundamental frequency, such that $t_0 - t_d \ll \omega(t)$.*

As illustrated in Fig.1, the proposed estimation scheme consists of two steps. In the first step, the frequency estimation problem is addressed, and subsequently, based on the frequency estimates, a kernel-based differentiator is designed to provide the estimates of the RoCoF. In both steps, the Volterra integral plays a key role, which is used to generate auxiliary signal images for identification. Respectively designed kernel functions are chosen respectively for each step to attain fast convergence properties. For readers' convenience, the foundations of the Volterra operator and the kernel functions are
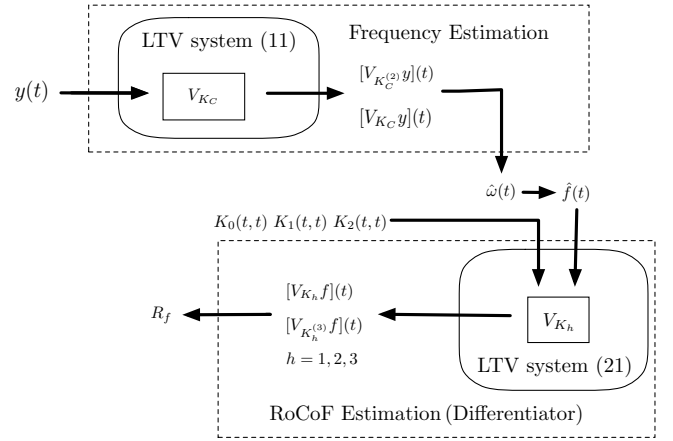
Fig. 1. Block diagram of the proposed estimation scheme.

provided in subsequence. More detailed introduction can be found in [16] and the reference therein.

The Volterra integral operator V_K with respect to a processed signal $y(t)$ is defined as $[V_K y](t) \triangleq \int_0^t K(t, \tau) y(\tau) d\tau, t \geq 0$, where $K(t, \tau)$ being a bivariate kernel that modulates the signal to achieve different estimation purpose. Moreover, in the rest of the paper, we denote the ith derivative of signal y as $y^{(i)}$ and the ith derivative of K with respect to the second argument by $K^{(i)}$. Furthermore, for a general kernel $K(t, \tau), \forall t > 0$, the Volterra image of a signal derivative admits the expansion

$$[V_K y^{(i)}](t) = \sum_{j=0}^{i-1} (-1)^{i-j-1} y^{(j)}(t) K^{(i-j-1)}(t, t)$$
$$+ \sum_{j=0}^{i-1} (-1)^{i-j} y^{(j)}(0) K^{(i-j-1)}(t, 0) + (-1)^i [V_{K^{(i)}} y](t), \tag{2}$$

which is instrumental to the following estimator design.

III. HIERARCHICAL ESTIMATION SCHEME

A. Frequency estimation scheme

Without loss of generality and to simplify the analysis, let the RoCoF changes start from the beginning such that $t_d = 0$. Taking the first derivative of the power signal (1), it holds that

$$y^{(1)}(t) = A\cos(\omega(t)t + \phi_0)\omega(t) + e_1(t), \tag{3}$$

where $e_1(t) \triangleq A\cos(\omega(t)t + \phi_0)\dot{\omega}(t)t$. It is worth noting that $e_1(t) \ll A\cos(\omega(t)t + \phi_0)\omega(t)$, for $t \leq t_0 \in \mathbb{R}_{\geq 0}$ under Assumption 2.

Moreover, the second derivative of $y(t)$ follows

$$y^{(2)}(t) = -A\sin(\omega(t)t + \phi_0)(\omega(t) + \dot{\omega}(t)t)^2 + A\cos(\omega(t)t + \phi_0)(2\dot{\omega}(t) + \ddot{\omega}(t)t), \tag{4}$$

which can be rearranged as

$$y^{(2)}(t) = y_{2m}(t) + e_2(t), \forall t \leq t_0. \tag{5}$$

with $y_{2m}(t) = -\omega(t)^2 y(t)$ and

$$e_2(t) = -(\dot{\omega}(t)^2 t^2 + 2\dot{\omega}(t)\omega(t)t) y(t) + A\cos(\omega(t)t + \phi_0)(2\dot{\omega}(t) + \ddot{\omega}(t)t) \tag{6}$$

and $y_{2m}(t) \gg e_2(t)$ for small $t \leq t_0 \in \mathbb{R}_{\geq 0}$.

By applying the Volterra integral V_{K_C} to both sides of (5) with respect to the kernel function K_C, we obtain

$$[V_{K_C}y^{(2)}](t) = [V_{K_C}y_{2m}](t) + [V_{K_C}e_2](t), \qquad (7)$$

where

$$K_C(t,\tau) = e^{-\rho(t-\tau)}(1 - e^{-\rho\tau})^N[1 - e^{-\rho(t-\tau)}]^N, \qquad (8)$$

tuned by the parameter $\rho > 0$ and $N = 2$. An advantageous feature of this specific kernel function is that, the corresponding operator of the signal derivatives $[V_{K_C}y^{(2)}](t)$ can be computed by the signal itself

$$[V_{K_C}y^{(2)}](t) = [V_{K_C^{(2)}}y](t). \qquad (9)$$

which can be inferred from (2). Furthermore, the ith derivative of the kernel (8) can be expressed in the following form

$$K_C^{(i)}(t,\tau) = e^{-\rho t}f_{i,1}(\tau) + e^{-2\rho t}f_{i,2}(\tau) + e^{-3\rho t}f_{i,3}(\tau)$$
$$\triangleq \sum_{j=1}^{3} K_{i,j}(t,\tau).$$

with $K_{i,j}(t,\tau) = e^{-j\rho t}f_{i,j}(\tau), i = 0, 2$. Due to the linearity of the integral operator, it follows that $\left[V_{K_C^{(i)}}y\right](t) = \sum_{q=1}^{3}\left[V_{K_{i,j}}y\right](t)$, where $\left[V_{K_{i,j}}y\right](t)$ can be calculated as the output of the following linear system

$$\begin{cases} \zeta_{i,j}^{(1)}(t) &= -j\rho\zeta_{i,j}(t) + K_{i,j}(t,t)y(t), \\ \left[V_{K_{i,j}}y\right](t) &= \zeta_{i,j}(t), \end{cases} \qquad (10)$$

with $\zeta_{i,j}(0) = 0$. As it can be noticed, the right-hand-side of (7) can be rewritten as

$$[V_{K_C}y_{2m}](t) + [V_{K_C}e_2](t) = -\omega(t)^2\left[V_{K_C}y\right](t) + \epsilon(t) \quad (11)$$

where $\epsilon(t)$ is a residual signal. In the following lines, we show that $\epsilon(t)$ is bounded by $\bar{\epsilon}$ that depends on M_1, M_2, A and t.

Let us first expand the residual $\epsilon(t)$, yielding $\epsilon(t) = [V_{K_C}e_2](t) + \epsilon_k(t)$, with $\epsilon_k(t) = [V_{K_C}y_{2m}](t) - (-\omega(t)^2[V_{K_C}y](t))$. In view of (6), it is easy to show that $e_2(t)$ is bounded by

$$|e_2(t)| \leq |(\dot{\omega}(t)^2t^2 + 2\dot{\omega}(t)\omega(t)t)y(t)|$$
$$+ |A\cos(\omega(t)t + \phi_0)(2\dot{\omega}(t) + \ddot{\omega}(t)t)|$$
$$\leq A\left(4\pi^2M_2^2t_0^2 + 2\pi(M_1M_2 + M_3)t_0 + 4\pi M_2\right) \triangleq \bar{e}_2.$$

for $t < t_0$. As $[V_{K_C}e_2](t)$ can be recast into the linear system (11) with e_2 being the input of the system, $[V_{K_C}e_2](t)$ is BIBO stable, such that there exists a $\bar{\epsilon}_e > 0$ depending on $M_1, M_2, A, \bar{e}_2$, such that $|[V_{K_C}e_2](t)| \leq \bar{\epsilon}_e, \forall t < t_0$. On the other hand, to characterize the boundedness of $\epsilon_k(t)$, we rearrange the kernel function (8) as

$$K_C(t,\tau) = (e^{-\rho\tau} - e^{\rho\tau} - 2)e^{-\rho t}$$
$$+ \left(4e^{\rho\tau} - 2e^{2\rho\tau} - 2\right)e^{-2\rho t} + \left(e^{\rho\tau} - e^{2\rho\tau} - e^{3\rho\tau}\right)e^{-3\rho t}$$

It holds that

$$[V_{K_C}y_{2m}](t) = e^{-3\rho t}\int_0^t\left(e^{\rho\tau} - e^{2\rho\tau} - e^{3\rho\tau}\right)y_{2m}(\tau)d\tau$$
$$+ e^{-2\rho t}\int_0^t\left(4e^{\rho\tau} - 2e^{2\rho\tau} - 2\right)y_{2m}(\tau)d\tau + e^{-\rho t}\int_0^t\left(e^{-\rho\tau} - e^{\rho\tau} - 2\right)y_{2m}(\tau)d\tau.$$

Taking the first term on the right-hand-side as an example, it can be rearranged as

$$e^{-\rho t}\int_0^t\left(e^{-\rho\tau} - e^{\rho\tau} - 2\right)y_{2m}(\tau)d\tau$$
$$= e^{-\rho t}\left[\left(\int_0^\tau\left(e^{-\rho s} - e^{\rho s} - 2\right)y(s)ds\right)\omega^2(\tau)\right]_0^t - \epsilon_1(t),$$

and it yields

$$|\epsilon_1(t)| = 2e^{-\rho t}\left|\int_0^t\left(\int_0^\tau\left(e^{-\rho s} - e^{\rho s} - 2\right)y(s)ds\right)\omega(\tau)\dot{\omega}(\tau)d\tau\right|$$
$$\leq 8\pi^2AM_1M_2e^{-\rho t}\left|\int_0^t\left(\int_0^\tau e^{-\rho s} - e^{\rho s} - 2\ ds\right)d\tau\right|$$
$$= 8\pi^2AM_1M_2\left|\frac{2 - 2e^{-\rho t} - 2\rho te^{-\rho t} - 2\rho^2t^2e^{-\rho t}}{\rho^2}\right|.$$

Following the same line of reasoning, one can conclude that

$$[V_{K_C}y_{2m}](t) = \omega(t)^2[V_{K_C}y](t) - \epsilon_k(t), \qquad (12)$$

where $\epsilon_k(t) = \epsilon_1(t) + \epsilon_2(t) + \epsilon_3(t)$

$$\epsilon_2(t) \triangleq 2e^{-2\rho t}\int_0^t\left(\int_0^\tau\left(4e^{\rho\tau} - 2e^{2\rho\tau} - 2\right)y(s)ds\right)\omega(\tau)\dot{\omega}(\tau)d\tau$$

$$\epsilon_3(t) \triangleq 2e^{-3\rho t}\int_0^t\left(\int_0^\tau\left(e^{\rho\tau} - e^{2\rho\tau} - e^{3\rho\tau}\right)y(s)ds\right)\omega(\tau)\dot{\omega}(\tau)d\tau.$$

Therefore, one can conclude that $\exists\ \bar{\epsilon} > 0$ depends on A, M_1, M_2 and ρ that bounds $|\epsilon(t)|$,

$$|\epsilon(t)| \triangleq |\epsilon_1(t) + \epsilon_2(t) + \epsilon_3(t) + \epsilon_e(t)| \leq \bar{\epsilon}.$$

From (7), (9) and (11), the following identity can be attained

$$[V_{K_C^{(2)}}y](t) = -\omega(t)^2\left[V_{K_C}y\right](t) + \epsilon(t), \qquad (13)$$

where both $[V_{K_C^{(2)}}y](t)$ and $[V_{K_C}y](t)$ can be calculated based on designed kernels and signal measurement $y(t)$. Given the residual $\epsilon(t)$ bounded and negligible for $t < t_0$, eliminating its effect in the following characterization can significantly reduce the computational complexity with a small compromise in the frequency estimation accuracy. However, the accuracy of RoCoF estimates, which is the key objective of the proposed work, can be guaranteed, as will be shown in the simulation. In this context, it is reasonable to estimate the angular frequency $\omega(t)$ by

$$\hat{\omega}(t) = \sqrt{-[V_{K_C^{(2)}}y](t)/\left[V_{K_C}y\right](t)} \qquad (14)$$

where $\hat{\omega}(t)$ represents the estimated frequency. The equation (14) may encounter a singularity issue when $[V_{K_C}y](t) = 0$. To avoid zero-crossing of the denominator, we apply the norm on both sides of (13), and after some rearrangements, it holds that

$$|[V_{K_C^{(2)}}y](t)| = \omega(t)^2|[V_{K_C}y](t)|.$$

By filtering both $|[V_{K_C^{(2)}}y](t)|$ and $|[V_{K_C}y](t)|$

$$\begin{aligned} \mathscr{L}[S_f(t)] &= F(s)\mathscr{L}\left\{\left|\left[V_{K_C^{(2)}}y\right](t)\right|\right\}, \\ \mathscr{L}[Z_f(t)] &= F(s)\mathscr{L}\{|[V_{K_C}y](t)|\}, \end{aligned} \qquad (15)$$

with $S_f(0) = 0$ and $Z_f(0) = 0$, the angular frequency is

estimated by

$$\hat{\omega}(t) = \begin{cases} \sqrt{S_f(t)/Z_f(t)}, & Z_f(t) > \sigma_1, \\ \hat{\omega}(0), & \text{otherwise} \end{cases} \quad (16)$$

where $\hat{\omega}(0)$ is the initial guess of the frequency, σ_1 is a user-defined threshold to ensure the invertibility of $Z_f(t)$. Given $\hat{\omega}(t)$, the frequency can be is identified by $\hat{f}(t) = \dfrac{\hat{\omega}(t)}{2\pi}$.

B. RoCoF Estimation Scheme

In order to track the RoCoF $R_f(t)$, a kernel-based differentiator [17] is deployed, with the frequency estimates $\hat{f}(t)$ as the input. Indeed, RoCoF estimation problem takes on the form of the state observation of following dynamic model

$$\dot{x}(t) = \begin{bmatrix} 0 & 1 & 0 \\ 0 & 0 & 1 \\ 0 & 0 & 0 \end{bmatrix} x(t) + \begin{bmatrix} 0 \\ 0 \\ e_{trun} \end{bmatrix}, \quad (17)$$

$$x(t) = \begin{bmatrix} f(t) & R_f(t) & \dot{R}_f(t) \end{bmatrix}^\top$$

and the $e_{trun}(t)$ is the truncation error which could be regarded as the disturbance. The 1st derivative of R_f is also modeled in the above system in order to enhance the robustness of the differentiator [17].

To achieve fast-convergent state estimation of the dynamic model (17), an array of another kind of Non-asymptotic Kernel are deployed, with the form

$$K_h(t,\tau) = e^{-\rho_h(t-\tau)} \left(1 - e^{-\bar{\rho}t}\right)^N, \quad (18)$$

sharing the same $\bar{\rho} \in \mathbb{R}_{>0}$ but with different $\rho_h \in \mathbb{R}_{>0}$, $h \in \{0, \ldots, N-1\}$.

For the given kernel function (18), it holds that

$$K_h^{(j)}(t,0) = 0, \forall j \in \{0, 1, \ldots, i-1\}, h \in \{0, 1, 2\},$$

and therefore, the Volterra image of signal derivatives induced by (18) verifies

$$\left[V_{K_h} f^{(i)}\right](t) = \sum_{j=0}^{i-1} (-1)^{i-j-1} f^{(j)}(t) K_h^{(i-j-1)}(t,t) + (-1)^i \left[V_{K_h^{(i)}} f\right](t).$$

Taking $i = 3$, the above equation becomes

$$\left[V_{K_h} f^{(3)}\right](t) = \omega(t) K_h^{(2)}(t,t) - R_f(t) K_h^{(1)}(t,t) + \dot{R}_f(t) K_h(t,t) - \left[V_{K_h^{(3)}} f\right](t).$$

Referring to (17), it holds that $\Gamma(t)x(t) = \mu(t)$, with

$$\Gamma(t) = \begin{bmatrix} K_0^{(2)}(t,t) & -K_0^{(1)}(t,t) & K_0(t,t) \\ K_1^{(2)}(t,t) & -K_1^{(1)}(t,t) & K_1(t,t) \\ K_2^{(2)}(t,t) & -K_2^{(1)}(t,t) & K_2(t,t) \end{bmatrix},$$

$$\mu(t) = \begin{bmatrix} -\left[V_{K_0^{(3)}} \omega\right](t), & -\left[V_{K_1^{(3)}} \omega\right](t), & -\left[V_{K_2^{(3)}} \omega\right](t) \end{bmatrix}^\top$$

The transformed signal vector $\mu(t)$, for $t \geq 0$, can be obtained as the output of the following LTV dynamic system:

$$\mu^{(1)}(t) = G\mu(t) + E(t)y(t), \quad (19)$$

with $\mu(0) = 0$,

$$G = \text{diag}\left(-\rho_0, -\rho_1, -\rho_2\right),$$

$$E(t) = \begin{bmatrix} K_0^{(3)}(t,t), K_1^{(3)}(t,t), K_2^{(3)}(t,t) \end{bmatrix}^\top.$$

By deploying the kernel (18), the invertibility of $\Gamma(t)$ is inherently guaranteed for all $t > 0$ [18]. In this connection, the state vector $x(t)$ can be immediately obtained as

$$\hat{x}(t) = \begin{bmatrix} \hat{\hat{f}}(t) \\ \hat{R}_f(t) \\ \hat{\dot{R}}_f(t) \end{bmatrix} = \begin{cases} 0, & \det\left(\Gamma(t)\right) > \sigma_2, \\ \Gamma^{-1}(t)\mu(t), & \det\left(\Gamma(t)\right) \geq \sigma_2, \end{cases} \quad (20)$$

in which σ_2 is a user-defined invertibility threshold to avoid large overshoot at the beginning. From (20), the real-time estimates of the RoCoF, $\hat{R}_f(t)$, is obtained. Moreover, it is worth noting that, $\hat{\hat{f}}(t)$ is the estimation of $\hat{f}(t)$, both can be used interchangeably.

IV. NUMERICAL VALIDATION

This section provides the numerical validation of the proposed approach. Three case studies are carried out, with two simulated power signals and an experimental signal generated by the testbench. In order to verify the robustness of the proposed algorithm, a random noise is added to power signal measurements in both cases with SNR = 40 dB.

For benchmarking purposes, the proposed algorithm is compared with a typical QPLL method in [6]. Both algorithms are implement in Matlab/Simulink environment with the sampling interval $T_s = 100$ μs. The kernel parameters are chosen as $\rho = 270$, $\bar{\rho} = 2.5$ and $[\rho_0, \rho_1, \rho_2] = [10, 20, 30]$, while the tuning parameters for QPLL are chosen as suggested by [6].

A. Simulation results

In this subsection, the performance of the proposed frequency and RoCoF estimators is evaluated, dealing with a power signal in the form of (1) with $A = 3$, $\phi_0 = \pi/3$. Moreover, the frequency $\omega(t)$ is subject to two typical modes of RoCoF variations, step changes and oscillatory changes [19].

1) Step change of RoCoF: In this scenario, we assume the RoCoF $R_f(t)$ follows the sequence $[0, 1, -1]$ Hz/s with each value holding for 2 seconds in order to emulate the inertia in reality. The performance of both estimation schemes are reported in Fig. 2 and Table I.
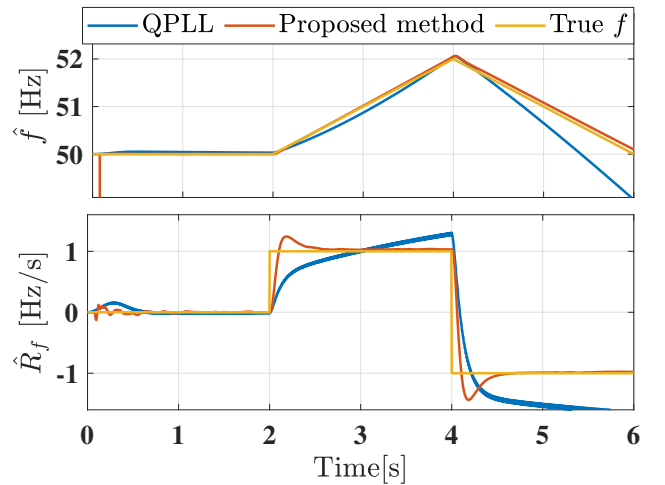
Fig. 2. Comparison between the kernel-based method and the QPLL method in the step-changing RoCoF scenario.

Time	RMSE	Kernel-based	QPLL
1st step	RMSE_f	1 p.u.	16.5241 p.u.
$[1,2]$s	RMSE_{R_f}	1 p.u.	3.8540 p.u.
2nd step	RMSE_f	1 p.u.	2.5727 p.u.
$[3,4]$s	RMSE_{R_f}	1 p.u.	5.2416 p.u.
3rd step	RMSE_f	1 p.u.	7.5885 p.u.
$[5,6]$s	RMSE_{R_f}	1 p.u.	36.2099 p.u.

It has been shown that the proposed scheme is able to estimate the frequency of signal subjected to RoCoF step changes. Although frequency changes are not perfectly tracked, the RoCoF estimation accuracy is not compromised. As shown by the RoCoF estimation results, overshoots occur at the beginning of each RoCoF step. However, they decay rapidly before the next RoCoF switching instant. In comparison with the QPLL, the proposed method shows improved tracking accuracy and converging speed.

Moreover, to provide further insight into the accuracy of both methods, the Root Mean Square Error (RMSE) over a specific time interval $[t_a, t_b]$ is evaluated by

$$\text{RMSE}_f \triangleq \sqrt{\frac{\sum_{i=k_a}^{N}\left(\hat{f}(i) - f(i)\right)^2}{N}},$$

$$\text{RMSE}_{R_f} \triangleq \sqrt{\frac{\sum_{i=k_a}^{N}\left(\hat{R}_f(i) - R_f(i)\right)^2}{N}},$$

where N represents the total number of data points taken for the calculation. k_a corresponds to the index of the time instant t_a. In Table I, the estimation RMSEs of both methods are compared concerning the steady state of each RoCoF steps ($t \in (1,2)$ s, $t \in (3,4)$ s and $t \in (5,6)$ s). The results show the significant performance improvement of the proposed method as compared to the QPLL method.

2) Oscillatory RoCoF: In this section, we consider an oscillatory RoCoF, and it profile follows the following expression

$$R_f(t) = 0.8e^{-0.2t}\sin\left(\pi t - \frac{\pi}{2}\right) + 0.4e^{-0.1t}\sin\left(0.6\pi + \frac{\pi}{6}\right).$$

The estimation results of the proposed RoCoF estimation scheme is presented in Fig. 3.

The estimation error $e_f(t) \triangleq |\hat{f}(t) - f(t)|$ tends to increase with time at beginning and tends to remain within a constant bound verifying the discussion of (11). Moreover, the estimation of RoCoF $\hat{R}_f(t)$ is fairly accurate with negligible latency. Remarkably, the RoCoF estimates track the true value with high convergence speed and no obvious latency can be observed.

The estimation results are compared with that of the QPLL as depicted in Fig. 4. The results are shown for the first 6 seconds for illustrative purposes. It is shown that the proposed estimation method is able to track the variation of the frequency with negligible convergence time and the frequency estimation error is kept within a tight bound, whereas the
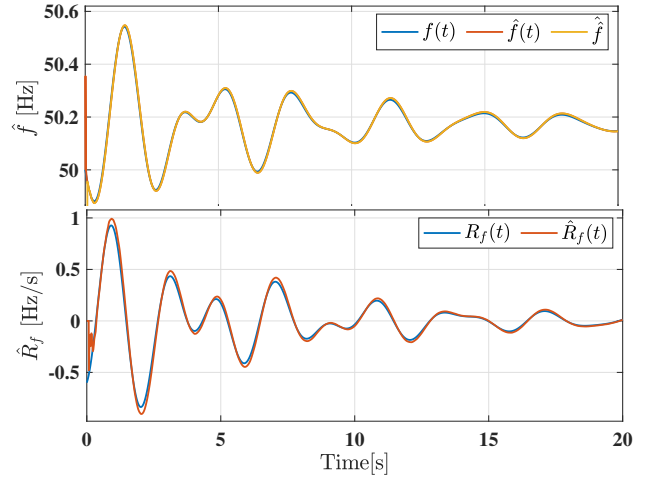
Fig. 3. Estimates of $f(t)$ and $R_f(t)$ in the continuous RoCoF scenario.
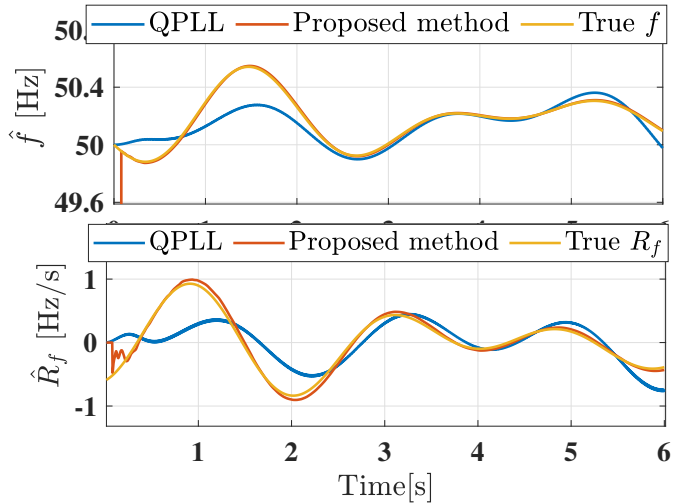
Fig. 4. Comparison between the kernel-based method and the QPLL method in the continuous RoCoF scenario.

QPLL is unable to provide reliable tracking for a time-varying frequency. Similar results can be found for the RoCoF estimation, the estimates generated by the kernel-based method show much more accurate tracking performance than the QPLL albeit oscillatory at the beginning due to the noise, and the influence of the noise vanishes at steady state.

The RMSEs of both methods are compared over both starting transient $[0.04, 0.5]$ s and the steady state $[10, 20]$ s, in order to quantify the estimation speed and accuracy. The listed estimation error shows that the proposed kernel-based method is able to achieve fast convergence without compromising steady state accuracy.

B. Results based on experimental data

In this section, a practical operating condition is established to emulate low inertia power system that usually arouses stability issues. A sudden frequency deviation is assumed to occur after the loss of generation, modeled as a step disturbance. To mitigate the potential instability, typical approaches, such as inertia emulation, rely significantly on prompt and accurate capture of the frequency and RoCoF. In this context, the effectiveness of the proposed scheme is evaluated under

Time	RMSE	Kernel-based	QPLL
Transient	$RMSE_f$	1 p.u.	16.7131 p.u.
$[0.04, 0.5]$s	$RMSE_{R_f}$	1 p.u.	6.1177 p.u.
Steady State	$RMSE_f$	1 p.u.	40.8055 p.u.
$[10, 20]$s	$RMSE_{R_f}$	1 p.u.	24.2624 p.u.
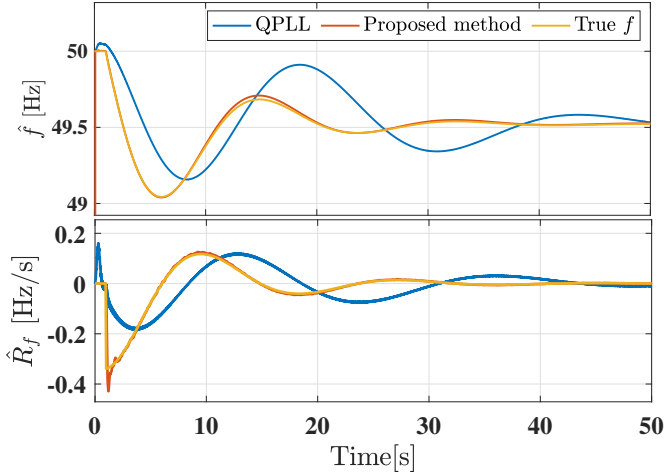
Fig. 5. Comparison between the kernel-based method and the QPLL method in the low inertia power system.

such conditions. The frequency evaluations, subject to the large disturbance, are generated based on the GB 2030 system with the total demand of $32\,\text{GW}$, after the loss of the largest generation $(1.8\,\text{GW})$ [20].

TABLE III
RMSE COMPARISON OF THE PROPOSED AND THE QPLL METHOD IN LOW
POWER ELECTRONICS PENETRATION SCENARIO.

Time	RMSE	Kernel-based	QPLL
Transient	$RMSE_f$	1 p.u.	35.8004 p.u.
$[1, 2]$s	$RMSE_{R_f}$	1 p.u.	2.9528 p.u.
Steady State	$RMSE_f$	1 p.u.	13.8517 p.u.
$[40, 50]$s	$RMSE_{R_f}$	1 p.u.	28.9568 p.u.

The estimation results are reported in Fig. 5 and Table III. It has been shown that the proposed estimation scheme can track the sudden frequency variation and retrieve its RoCoF under such a practical condition. Remarkably, no visible latency has been shown in the results of the proposed method which is obvious in the results of the QPLL method. Moreover, as being confirmed by the RMSE in Table III, the proposed method possesses advantageous accuracy during the initial transient when strategies like emulated inertia are vitally valuable for stability control.

V. CONCLUSION

In this paper, a novel estimation scheme is proposed to track the frequency and the RoCoF of frequency-varying signals in the power systems. The scheme is composed of two fast-convergent estimators in series. The key element of the estimators is the Volterra integral operator, which ensures enhanced convergence rate and accuracy as compared to the QPLL. Moreover, the well-known trade-off between the estimation accuracy and latency, commonly existing in several recent works, can be mitigated. Typical scenarios in power systems are simulated validating the performance of the proposed method.

REFERENCES

[1] D. W. P. Thomas and M. S. Woolfson, "Evaluation of frequency tracking methods," *IEEE Transactions on Power Delivery*, vol. 16, no. 3, pp. 367–371, 2001.

[2] L. Hsu, R. Ortega, and G. Damm, "A globally convergent frequency estimator," *IEEE Transactions on Automatic Control*, vol. 44, no. 4, pp. 698–713, April 1999.

[3] M. Mojiri and A. R. Bakhshai, "An adaptive notch filter for frequency estimation of a periodic signal," *IEEE Transaction on Automatic Control*, vol. 49, no. 2, pp. 314–318, February 2004.

[4] B. Wu and M. Bodson, "A magnitude/phase-locked loop approach to parameter estimation of periodic signals," *IEEE Transactions on Automatic Control*, vol. 48, no. 4, pp. 612–618, April 2003.

[5] M. Karimi-Ghartemani and A. K. Ziarani, "A nonlinear time-frequency analysis method," *IEEE Transactions on Signal Process*, vol. 52, no. 6, pp. 1585–1595, June 2004.

[6] H. Karimi, M. Karimi-Ghartemani, and M. R. Iravani, "Estimation of frequency and its rate of change for applications in power systems," *IEEE Transactions on Power Delivery*, vol. 19, no. 2, pp. 472–480, 2004.

[7] A. K. Singh and . B. C. Pal, "Rate of change of frequency estimation for power systems using interpolated dft and kalman filter," *IEEE Transactions on Power Systems*, vol. 34, no. 4, pp. 2509–2517, 2019.

[8] D. Belega, D. Fontanelli, and D. Petri, "Dynamic phasor and frequency measurements by an improved taylor weighted least squares algorithm," *IEEE Transactions on Instrumentation and Measurement*, vol. 64, no. 8, pp. 2165–2178, August 2015.

[9] H. Ahmed, S. Amamra, and I. Salgado, "Fast estimation of phase and frequency for single-phase grid signal," *IEEE Transactions on Industrial Electronics*, vol. 66, no. 8, pp. 6408–6411, August 2019.

[10] J. R. Trapero, H. Sira-Ramirez, and V. F. Battle, "An algebraic frequency estimator for a biased and noisy sinusoidal signal," *Signal Processing*, vol. 87, no. 6, pp. 1188–1201, 2007.

[11] ——, "On the algebraic identification of the frequencies, amplitudes and phases of two sinusoidal signals from their noisy sum," *International Journal of Control*, vol. 81, no. 3, pp. 507–518, 2008.

[12] G. Fedele and L. Coluccio, "A recursive scheme for frequency estimation using the modulating function method," *Applied Mathematics and Computation*, vol. 216, no. 5, pp. 1393–1400, 2010.

[13] B. Chen, P. Li, G. Pin, G. Fedele, T. Parisini, and S. R. Hui, "Finite-time estimation of multiple exponentially-damped sinusoidal signals: A kernel-based approach," *Automatica*, vol. 106, pp. 1–7, 2019.

[14] G. Pin, A. Assalone, M. Lovera, and T. Parisini, "Non-asymptotic kernel-based parametric estimation of continuous-time linear systems," *IEEE Transactions on Automatic Control*, vol. 61, no. 2, pp. 360–373, 2016.

[15] G. Pin, M. Lovera, A. Assalone, and T. Parisini, "Kernel-based non-asymptotic state estimation for linear continuous-time systems," in *2013 American Control Conference*, 2013, pp. 3123–3128.

[16] P. Li, "Finite-time system identification, estimation and fault detection," *Imperial College London*, pp. 1–137, 2019.

[17] P. Li, G. Pin, G. Fedele, and T. Parisini, "Non-asymptotic numerical differentiation: a kernel-based approach," *International Journal of Control*, vol. 91, no. 9, pp. 2090–2099, 2018.

[18] P. Li, F. Boem, G. Pin, and T. Parisini, "Kernel-based simultaneous parameter-state estimation for continuous-time systems," *IEEE Transactions on Automatic Control*, vol. 65, no. 7, pp. 3053–3059, 2020.

[19] N. Jenkins, "Impact of dispersed generation on power systems," *Electra*, vol. 199, pp. 6–13, 2001.

[20] Z. Chu, U. Markovic, G. Hug, and F. Teng, "Towards optimal system scheduling with synthetic inertia provision from wind turbines," *IEEE Transactions on Power Systems*, vol. 35, no. 5, pp. 4056–4066, 2020.